Adsorbate-Induced Rayleigh-Phonon Gap of $p(2\times2)$O/Pt(111)

Klaus Kern, Rudolf David, Robert L. Palmer, and George Comsa
Institut für Grenzflächenforschung und Vakuumphysik, Kernforschungsanlage Jülich, D-5170 Jülich, West Germany

and

Jin He and Talat S. Rahman
Department of Physics, Kansas State University, Manhattan, Kansas 66506
(Received 19 February 1986)

The dispersion of the vibrational modes of the $p(2\times2)$O/Pt(111) system has been measured by inelastic He scattering along the $\bar{\Gamma}\bar{M}$ azimuth. The experimental results show the first direct evidence for the appearance of an energy gap in the Rayleigh curve at the $p(2\times2)$ reduced-zone boundary. Both the size of the gap (~ 0.85 meV) and the appearance of a new mode near the $\bar{\Gamma}$ point are reproduced by a lattice-dynamical analysis, if three-body interactions of the bond-stretching type are included in the calculations.

PACS numbers: 68.35.Ja, 63.20.Dj, 79.20.Rf

The presence of ordered monolayers of chemisorbed atoms and molecules on metal surfaces modifies the substrate Rayleigh-phonon dispersion curve even in the absence of surface reconstruction. Experimental results reported so far show that, in spite of substantial quantitative changes, the shape of the Rayleigh curve remains qualitatively unchanged.[1] However, it has been predicted theoretically[2,3] that also qualitative changes, like the opening of an energy gap at the new zone boundary, might appear. Because of its very high resolution, He inelastic scattering[4] is the method to be used to uncover such an effect.

We report here the first observation of an adsorbate-induced energy gap in the surface Rayleigh curve. The data are obtained by high-resolution inelastic He scattering from a $p(2\times2)$ oxygen overlayer on Pt(111). The measured surface phonon dispersion is compared with lattice-dynamical calculations. The size of the experimental gap (~ 0.85 meV) can be reproduced if three-body interactions between adsorbate and substrate atoms are included.

The components of the experimental setup, nozzle beam source, target chamber, and differentially pumped time-of-flight (TOF) spectrometer, have been described in detail somewhere else.[5,6] Here only the features relevant for this experiment will be given. The total scattering angle is fixed, i.e., $\vartheta_i+\vartheta_f=90°$. Incident He beam energies in the range $10<E_{\rm He}<35$ meV are used; the velocity spread is $\Delta v/v\approx 0.8\%$. The overall effective energy resolution upon cross-correlation analysis of the TOF distribution is about 0.3 meV (FWHM). Both the angular spread of the incident beam and the angle subtended by the ionizer opening are equal to 0.2°, i.e., the effective angular resolution is 0.3°. The Pt(111) crystal is mounted on a manipulator in a UHV chamber with a base pressure in the low 10^{-11} Torr range. The Pt(111) surface is obtained by careful orientation, cutting, and polishing.[7] Repeated sputtering, oxygen and thermal cleaning, as well as annealing cycles finally yield a surface with a defect density less than 0.1%.[8] All measurements reported here are performed in the $\langle 11\bar{2}\rangle$ crystal direction ($\bar{\Gamma}\bar{M}$ in the reciprocal space). The azimuthal alignment of the crystal is based on the position of the $(\bar{1},\bar{1})_{\rm Pt}$ diffraction peak (Fig. 1). The $p(2\times2)$ oxygen overlayer is obtained by exposing the crystal ($T_s=300$ K) to molecular oxygen. The saturation coverage $\theta_s\approx 0.25$ corresponds to a peak-to-peak ratio of $I_{\rm O,510}/I_{\rm Pt,237}\approx 0.4$ in the Auger spectrum ($E=2000$

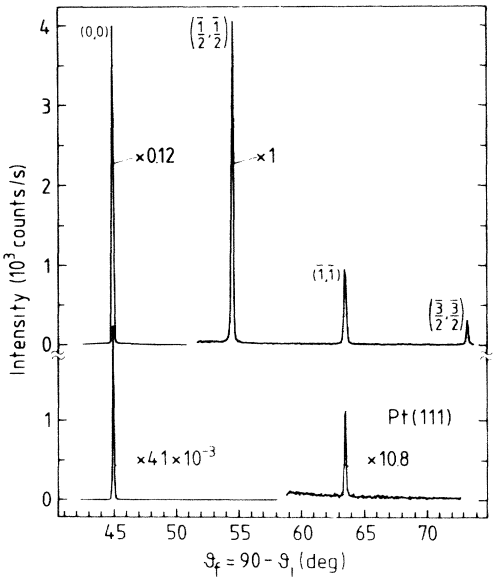

FIG. 1. He polar diffraction patterns in the $\langle 11\bar{2}\rangle$ direction from the clean (bottom) and $p(2\times2)$O/Pt(111) surface (top). $E_{\rm He}=17.3$ meV, $T_s=300$ K.

eV). Sharp $p(2\times2)$ LEED and He-diffraction patterns with low background are observed. In Fig. 1 the He polar scans of the clean and $p(2\times2)$O/Pt(111) surface are shown. Under the given vacuum conditions, no contamination or depletion (by reaction with CO or H_2) of the oxygen overlayer is observed during several hours. The diffraction pattern in Fig. 1 measured in the $\langle 11\bar{2}\rangle$ direction together with similar patterns in the $\langle 1\bar{1}0\rangle$ direction show that the oxygen overlayer forms a $p(2\times2)$ structure. The hardly noticeable increase in peak width with respect to the patterns from the clean Pt surface (domain size >2000 Å)[8] indicates that the size of the well-ordered $p(2\times2)$O domains is about 400 Å.

The intensity ratio of the first- to the zero-order diffraction peak in Fig. 1 is ~ 150 times larger for the $p(2\times2)$O surface than for the clean one as a result of the much larger corrugation of the He-surface potential. As a consequence, inelastic events involving reciprocal lattice vectors, $\mathbf{G}_{ij}$, with $i,j\neq0$ also become probable. This can be seen clearly in the time-of-flight plots in Fig. 2 measured for He atoms scattered from the clean and the $p(2\times2)$O/Pt(111) surface under identical conditions. The $\vartheta_i = 51°$ and 42.4° clean-surface plots show either energy-gain (phonon annihilation) or energy-loss (phonon creation) features, respectively.[9] In contrast, the $p(2\times2)$O surface plots are much richer. Besides annihilation and creation features with $\mathbf{G}_{00}=0$, the plots also show creation and annihilation peaks with $\mathbf{G}_{11}\neq0$.

Out of more than 40 TOF plots like those in Fig. 2 the experimental Rayleigh-phonon dispersion curve of the $p(2\times2)$O/Pt(111) surface is constructed [Fig. 3(a)]. Because of the periodicity imposed by the oxygen layer, the length of the reduced Brillouin zone of the $p(2\times2)$O surface is half that of clean Pt(111) ($\bar{\Gamma}\bar{M}_O = \frac{1}{2}\bar{\Gamma}\bar{M}_{Pt}$). The TOF spectra are measured at three different incident He-beam energies (10.0, 17.4, and 35.0 meV). No systematic influence of this parameter is observed.

The data in Fig. 3(a) demonstrate clearly the existence of an energy gap of (0.85 ± 0.2) meV at the $\bar{M}_O$ point. This is the first time that such a gap induced by an adsorbed layer in the Rayleigh curve is observed experimentally. Another feature induced by the adsorbate is the appearance of a mode near the $\bar{\Gamma}$ point. Note that this mode is observed only for inelastic events involving $\mathbf{G}_{00}=0$ (open circles).

As already mentioned, the opening of an energy gap in the Rayleigh curve due to the presence of an adlayer has been predicted theoretically.[2,3] Even an elementary argument makes this plausible. The elementary cell of the $p(2\times2)$O/Pt(111) surface contains four Pt and one O atom (see, e.g., Fig. 4). If we assume, as usual, that the O atom sits in a threefold hollow site, three Pt atoms are "loaded" with one O atom, while the fourth Pt atom is not. This excess loading leads to an energy gap at the $\bar{M}_O$ point (similar to the textbook "two mass chain" case). A dynamical calculation involving only central forces, which has been successful in reproducing the clean-Pt(111)-surface Rayleigh curve,[9] leads to an energy gap smaller than 0.1 meV.[10]

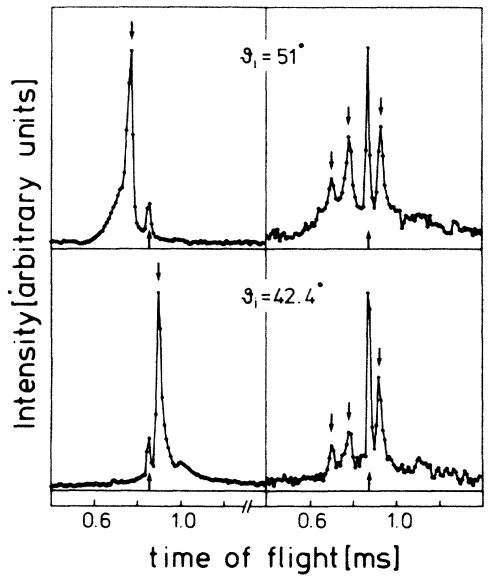

FIG. 2. He TOF plots taken in the $\bar{\Gamma}\bar{M}$ direction from the clean (left) and the $p(2\times2)$O/Pt(111) surface (right). $E_{He}=17.4$ meV, $T_s=300$ K. The diffuse elastic peaks are denoted by arrows pointing up.

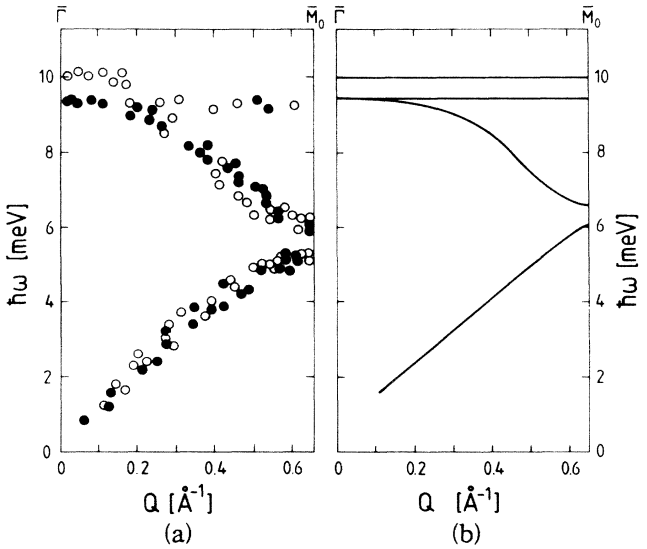

FIG. 3. (a) Experimental and (b) theoretical Rayleigh-phonon dispersion curves of the $p(2\times2)$O/Pt(111) surface, in the $\bar{\Gamma}\bar{M}_O$ direction, reduced to the first Brillouin zone. The phonon events belonging to the first Brillouin zone are denoted by open circles while those belonging to the second zone (i.e., involving $\mathbf{G}_{11}$), by filled circles.

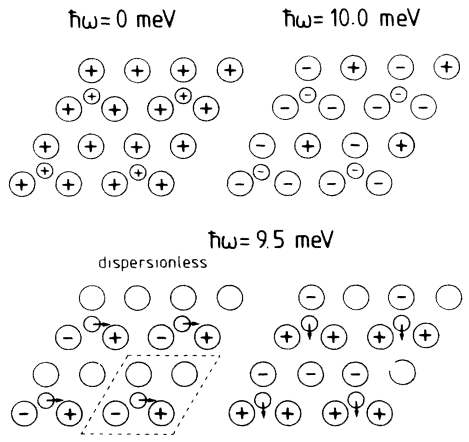

FIG. 4. Sketch of the four eigenmodes of the $p(2\times2)$O/Pt(111) surface as they result from the dynamical analysis at the $\bar{\Gamma}$ point.

Even the assumption that the fourth, non-O-loaded Pt atom couples differently to the second-layer Pt atoms than the three O-loaded Pt atoms does not lead to the experimental gap value except for some particular force-constant combinations. Unfortunately, these particular conditions generate additional modes spread throughout the whole Brillouin zone between 6 and 10 meV; these are not seen in the experiment.[10]

In order to investigate whether a more realistic lattice-dynamical model reproduces the size of the experimental energy gap, we have introduced in our calculations besides nearest-neighbor central forces also an additional noncentral force of the bond-stretching type between adsorbate and the nearest-neighbor substrate atoms. It was recently found that such noncentral forces play an important role in the case of $p(2\times2)$ structures.[11,12] [For the higher-coverage $c(2\times2)$ structure forces of this type cancel out.]

Our lattice-dynamical Hamiltonian then has the following additional term

$$V_{\beta s}=\tfrac{1}{2}k'\sum_{i\neq j}\Delta l_i\,\Delta l_j, \tag{1}$$

where

$$\Delta l_i=\hat{\mathbf{n}}_{0i}\cdot[\mathbf{u}(i)-\mathbf{u}(0)] \tag{2}$$

with $\hat{\mathbf{n}}_{0i}$ being the unit vector from the adsorbate atom to the first-layer substrate atom i and $\mathbf{u}(i)$ and $\mathbf{u}(0)$ the displacements of the substrate and the adsorbate atom, respectively. This term correlates the stretching of two Pt—O bonds, thereby introducing a three-body interaction between the adsorbate and substrate atoms. This affects not only the dispersion of the adsorbate modes but also that of the substrate phonons. Potential-energy contributions of the type above are frequently found in the literature on the vibrations of large molecules where it is more convenient to work in the internal coordinates of the molecule. For our purposes we transform these internal coordinates into Cartesian ones and the potential energy into a form more amenable to lattice-dynamical analysis. This can be done quite easily by substituting Eq. (2) into Eq. (1) and reminding ourselves that the potential-energy term has the general form[13]

$$V=\tfrac{1}{2}\sum_{\alpha\beta ij}\Phi''_{\alpha\beta}(ij)u_\alpha(i)u_\beta(j), \tag{3}$$

where $\Phi''_{\alpha\beta}(ij)$ is the second derivative of the pair potential between atoms and α,β denote Cartesian coordinates. A comparison of the bond-stretching–interaction terms with Eq. (3) gives us the contribution to the pair potential and subsequently the new terms in the dynamical matrices. A detailed analysis of this noncentral force and the ensuing lattice-dynamical analysis has been presented elsewhere.[12,13]

The calculations of the phonon dispersion curves are performed for a slab of twenty layers with use of standard computer programs to diagonalize the resulting dynamical matrix to obtain the eigenvalues and eigenvectors. Since experimental results are confined to the lower-frequency modes, we plot in Fig. 3(b) the dispersion of only those modes. We assume that the adsorbate sits at 1.38 Å above the Pt(111) surface and that the Pt-O force constant is 1.85×10^5 dyn/cm in order to give an oxygen-Pt stretch frequency of 59 meV.[14] For the intralayer and interlayer Pt-Pt force constants we choose the values which lead to the best fit of the whole set of clean Pt(111) data,[15] i.e., $k_{11}=0.4k$ and $k_{12}=1.1k$ with k the Pt bulk force constant. The bond-stretching force constant $k'=-2.31\times10^4$ dyn/cm gives the best fit.

The comparison between theory and experiment in Fig. 3 shows that by introduction of noncentral forces between adsorbate and substrate atoms the size of the energy gap at the $\bar{M}_0$ point is reasonably reproduced [0.5 meV to (0.85 ± 0.2) meV]. The middle of the gap predicted theoretically lies ~0.5 meV higher than the experimental one. The calculations also predict the observed new mode near the $\bar{\Gamma}$ point. It is a dispersionless mode with $\hbar\omega=10.0$ meV, which is, however, seen only in one-quarter of the Brillouin zone. There is also an additional dispersionless mode at $\hbar\omega=9.5$ meV which merges with the optical branch of the Rayleigh wave near the Γ point. This dispersionless mode appears to be present in the whole zone even if with low-intensity peaks. All four eigenmodes at the $\bar{\Gamma}$ point are plotted in Fig. 4. In all cases the eigenvectors of the substrate atoms are mainly vertically polarized. The eigenvectors of the adsorbate are horizontally polarized in the 9.5-meV modes and vertically in the acoustical and in the 10-meV modes.

It is interesting that although horizontally polarized modes have not been observed so far by He scattering, we do see in the present experiment the modes in which the O eigenvectors are horizontally polarized. It is probable that, although the scattering potential is mainly determined by the O atoms, the top-layer Pt atoms (which are vertically polarized) contribute enough to this potential so that these modes are also excited. The comparison with the experiment near the $\bar{\Gamma}$ point in Fig. 3(a) leads to an unexpected finding. The optical mode with vertically polarized adsorbate eigenvector is seen only for events with $\mathbf{G}_{00}=0$, not for those with $\mathbf{G}_{11}\neq 0$; for the optical modes with horizontally polarized adsorbate eigenvectors the opposite is true near the $\bar{\Gamma}$ point. We have, so far, no real explanation for this interesting effect.

In summary, the Rayleigh-phonon dispersion curve of Pt(111) undergoes two main modifications by the presence of an ordered $p(2\times 2)$O layer: the opening of an energy gap of (0.85 ± 0.2) meV at the $\bar{M}_O$ point and the appearance of a new mode near the $\bar{\Gamma}$ point. The size of the gap and the mode are reproduced by a lattice-dynamical analysis only if a noncentral force between adatoms and top-layer Pt atoms is included. The involvement of the reciprocal lattice vectors in the scattering process appears to have a substantial and so far unexpected influence on the phonon excitation probabilities.

Illuminating discussions with Harald Ibach and the communication of theoretical central-force results by John Black were of invaluable help and are gratefully acknowledged.

[1]J. M. Szeftel, S. Lehwald, H. Ibach, T. S. Rahman, J. E. Black, and D. L. Mills, Phys. Rev. Lett. **51**, 268 (1983).

[2]L. Dobrzynski and D. L. Mills, Phys. Rev. B **7**, 1322 (1973).

[3]L. Dobrzynski, G. Allan, B. Djafari-Rouhani, and B. K. Agrawal, in *Vibrational Spectroscopy of Adsorbates,* edited by R. F. Willis, Springer Series in Chemical Physics Vol. 15 (Springer-Verlag, Berlin, 1980), p. 55.

[4]J. P. Toennies, J. Vac. Sci. Technol. A **2**, 1055 (1984).

[5]K. Kern, R. David, and G. Comsa, Rev. Sci. Instrum. **56**, 369 (1985).

[6]G. Comsa, R. David, and B. J. Schumacher, Rev. Sci. Instrum. **52**, 789 (1981).

[7]U. Linke and B. Poelsema, J. Phys. E **18**, 26 (1985).

[8]B. Poelsema, R. L. Palmer, G. Mechtersheimer, and George Comsa, Surf. Sci. **117**, 60 (1982).

[9]K. Kern, R. David, and G. Comsa, Surf. Sci. **164**, L831 (1985). We have shown in this paper that by choosing appropriate scan curves, creation *and* annihilation events can be seen on the same TOF plot. However, in Fig. 2 here these conditions are not met.

[10]J. Black, private communication.

[11]K. G. Lloyd and J. C. Hemminger, Surf. Sci. **143**, 509 (1984).

[12]J. He and T. S. Rahman, to be published.

[13]T. S. Rahman, J. E. Black, and D. L. Mills, Phys. Rev. B **25**, 883 (1982).

[14]H. Steininger, S. Lehwald, and H. Ibach, Surf. Sci. **123**, 1 (1982).

[15]K. Kern, R. David, R. L. Palmer, G. Comsa, and T. S. Rahman, to be published.